Supplement of Atmos. Chem. Phys., 22, 14825–14836, 2022
https://doi.org/10.5194/acp-22-14825-2022-supplement


Atmospheric Chemistry and Physics
Open Access
EGU

*Supplement of*

# Constraining the particle-scale diversity of black carbon light absorption using a unified framework

**Payton Beeler and Rajan K. Chakrabarty**

*Correspondence to:* Rajan K. Chakrabarty (chakrabarty@wustl.edu) and Payton Beeler (beelerpayton@wustl.edu)

**Data from field and laboratory experiments**

*Cappa, et al. 2012.*

The mixing state of internally mixed BC aggregates measured by Cappa *et al.* 2012 (1) was found by first fitting a power-law function to mean $R_{BC}$ as function of photochemical age (-log([$NO_x$]/[$NO_y$])), which is shown in figure 1(a). The fitted equation is given by:

$$R_{BC} = (12.215 \pm 0.396)\left(-\log\left(\frac{[NO_x]}{[NO_y]}\right)\right)^{0.554 \pm 0.067}. \quad \text{(S1)}$$

Mass absorption cross-section of BC ($MAC_{BC}$) at wavelength ($\lambda$) of 532 nm is then calculated from figure S-17 of Cappa *et al.* 2012, which shows $MAC_{BC}$ enhancement ($E_{abs}$) as a function of photochemical age. Photochemical age was converted to $R_{BC}$ using equation S1, and $E_{abs}$ was converted to $MAC_{BC}$ using the reported value for $MAC_{BC}$ of pure BC (7.75 $m^2/g$). The morphology of particles from this study was inferred using lognormal fits of the size distributions given in figure S-13 of Cappa *et al.* 2012. The single particle BC mass was then calculated assuming BC density of 1.8 $g/cm^3$ (2).

*Saliba, et al. 2016.*

Measured $MAC_{BC}$ as a function of BC mixing state was taken from Figure 4 of Saliba *et al.* 2016 (3). The mixing state was then converted from organic to black carbon mass ratio (OA:BC) to $R_{BC}$ using:

$$R_{BC} = \text{OA:BC}. \quad \text{(S2)}$$

The morphology of particles from this study was inferred using lognormal fits of the size distributions given in figure S9 of Saliba *et al.* 2019. The single particle BC mass was then calculated assuming BC density of 1.8 $g/cm^3$ (2).

*Xie, et al. 2019.*

Measured $E_{abs}$ as a function of $R_{BC}$ was taken from Figure 1a of Xie *et al.* 2019 (4). enhancement was converted to $MAC_{BC}$ using a reference $MAC_{BC}$ value of 6.55 $m^2/g$ at $\lambda$ = 630 nm, given that the authors state that the thermodenuder-derived $E_{abs}$ was well correlated with $E_{abs}$ calculated using reference $MAC_{BC}$ (4).

*Cui, et al. 2016.*

Measured $E_{abs}$ as a function of BC mixing state was taken from Figure 5c of Cui *et al.* 2016 (5). The mixing state was converted from organic to elemental carbon ratio (OC/EC) to $R_{BC}$ using:

$$R_{BC} = \text{OC/EC}. \quad \text{(S3)}$$

Absorption enhancement was converted to $MAC_{BC}$ using $MAC_{BC}$ of pure BC = 4.02 $m^2/g$ at $\lambda$ = 678 nm, given in figure 2 of Cui *et al.* 2016 (5).

*Denjean, et al. 2020.*

Measured $E_{abs}$ as a function of BC mixing state was taken from Figure 2 of Denjean *et al.* 2020 (6). Absorption enhancement was converted to $MAC_{BC}$ using $MAC_{BC}$ of pure BC = 7.7 $m^2/g$ at $\lambda$ = 550 nm. The morphology of particles from this study was inferred using lognormal fits of the size distributions given in figure 1 of Denjean *et al.* 2020. The average mass was then calculated assuming BC density of 1.8 $g/cm^3$ (2).

*Zanatta, et al. 2018.*

Average $MAC_{BC}$ and $R_{BC}$ were found using reported values for average coating thickness, coating density, and $MAC_{BC}$ in Zanatta et al. 2018 (7). The morphology of particles from this study was inferred using reported size distributions given in Table 2 of Zanatta *et al.* 2018. The single particle BC mass was then calculated assuming BC density of 1.8 $g/cm^3$ (2).

*Liu, et al. 2015.*

Measured $MAC_{BC}$ as a function of BC mixing state was taken from Figure S2 of Liu *et al.* 2015 (8). We utilize $MAC_{BC}$ derived using standardized major axis at $\lambda$ = 781 nm in order to avoid potential influence of absorbing coatings on $MAC_{BC}$. The morphology of particles from this study was inferred using the limits of BC diameter given in Figure 1d of Liu *et al.* 2015. The single particle BC mass was then calculated assuming BC density of 1.8 $g/cm^3$ (2).

*Cappa, et al. 2019.*

Measured $MAC_{BC}$ as a function of BC mixing state was taken from Figure S4 and S6 of Cappa *et al.* 2019 (9). We analyze measurements of $MAC_{BC}$ at $\lambda$ = 532 nm only.

*Shiraiwa, et al. 2010.*

Measured $E_{abs}$ as a function of BC mixing state was taken from Figure 2 of Shiraiwa *et al.* 2010 (10). The mixing state was converted from the ratio of total particle diameter to black carbon diameter using BC density of 1.8 g/cm$^3$ and coating density of 1.2 g/cm$^3$ (2). The morphology of particles from this study was inferred using reported BC core diameter.

*Zhang, et al. 2018.*

Measured $E_{abs}$ as a function of BC mixing state was taken from Figure S3 of Zhang *et al.* 2018 (11). The mixing state was converted from organic to elemental carbon mass ratio to $R_{BC}$ using equation S3. Absorption enhancement was converted to $MAC_{BC}$ using $MAC_{BC}$ of pure BC = 4.7 m$^2$/g at $\lambda$ = 880 nm. The morphology of particles from this study was inferred using the reported range of BC core diameters (100-150 nm).

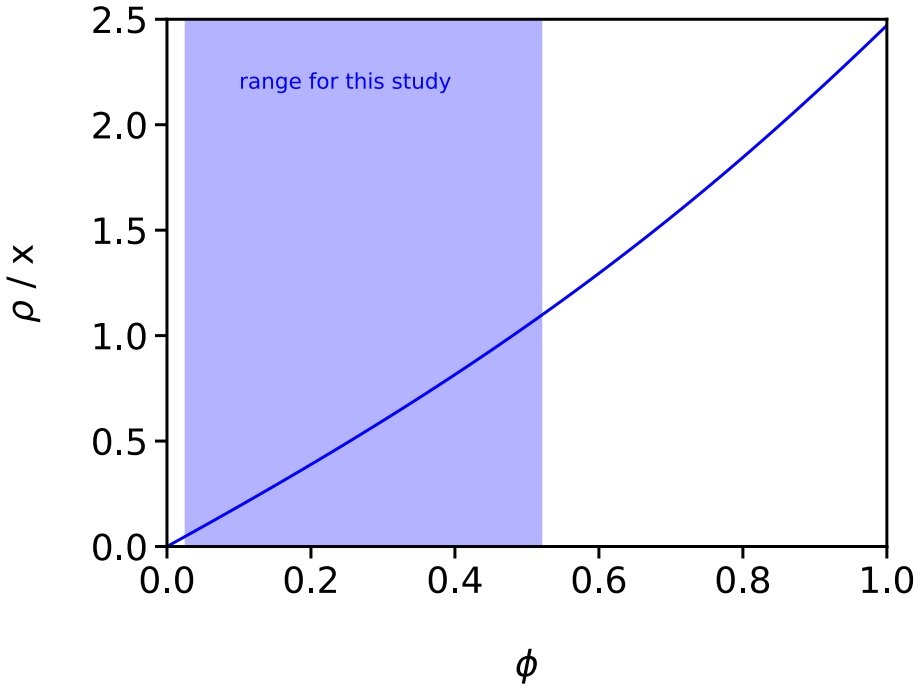


**Figure S1: Size parameter normalized phase shift parameter of black carbon as a function of monomer packing fraction. The shaded area represents the range of monomer packing fraction for aggregates in this study.**

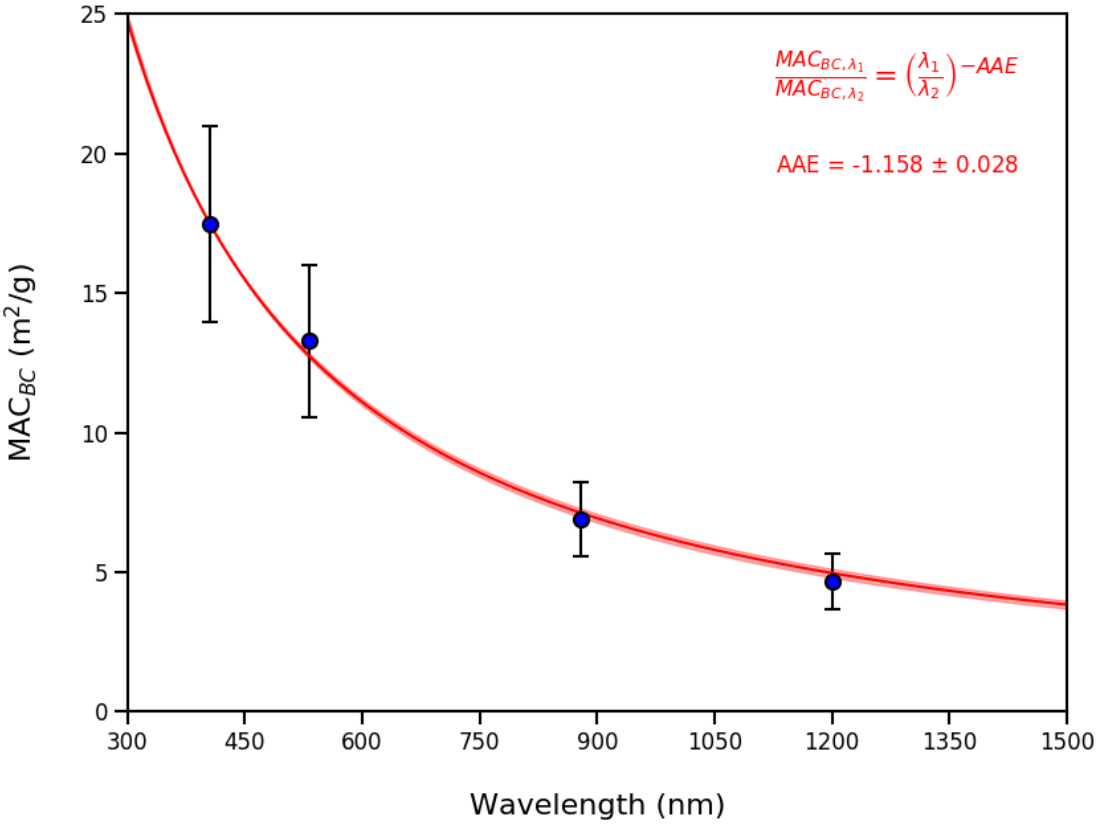


**Figure S2: Data used to calculate AAE for fractal BC aggregates with $\rho_{BC} \leq 1$, error bars show one standard deviation. Solid line shows fitted equation given in figure, error of AAE is reflective of 95% confidence interval.**

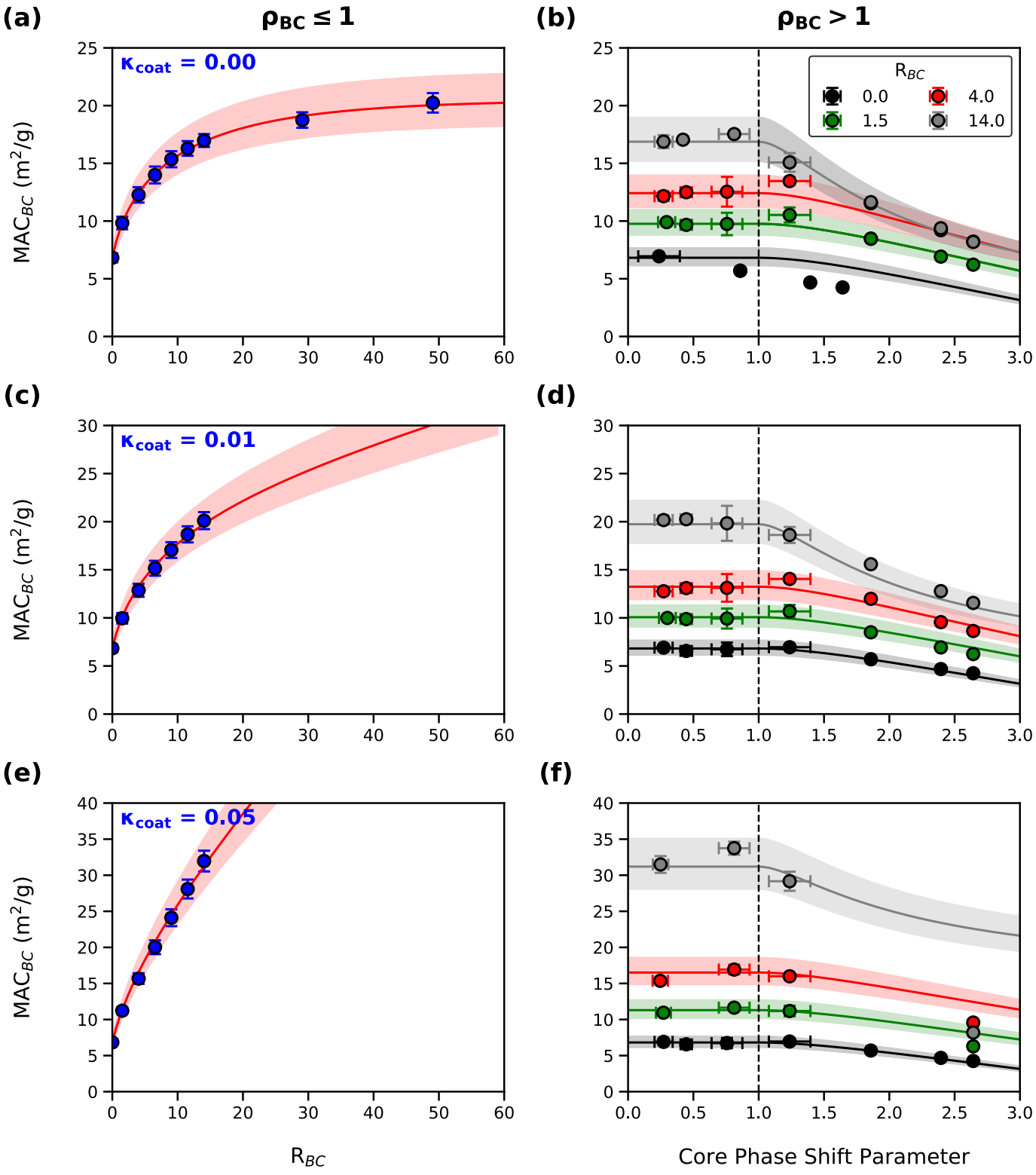


80

**Figure S3: $MAC_{BC}$ as a function of RBC and $\rho_{BC}$ with shaded areas representing the range of $MAC_{BC}$ assuming BC density of 1.6 g/cm$^3$ – 1.8 g/cm$^3$.**